

On modelling of thermal radiation properties for biofuels

T. K. Nilsson & B. Sundén
Lund Institute of Technology, Sweden

Abstract

Simple and computer attractive models for calculating radiation properties are needed. This paper considers recent models available in literature, and provides suggestions how to improve the calculation performance of the existing ones.

1 Introduction

Absorbing gases (H_2O , CO_2 , CO and CH_4) and soot particles (small particles) are formed when biofuels are burnt. Further, large particles in a fixed bed, if a fixed bed combustor is considered, influence the radiative heat transfer. The properties needed for thermal radiation calculation are of crucial importance for the result of the radiation calculations. Therefore, the gas absorption coefficient, and the particles absorption and scattering coefficients, need to be modelled as accurately as possible. Accurate predictions usually mean more involved models that need more computational time. The use of such models can make the radiation calculations the most time consuming part in CFD analyses. Simple and less computer intensive, but still useful, expressions are presented in this paper.

2 Large particle absorption and scattering coefficients

The absorption coefficient of large particles like wood particles, i.e., not soot like particles, is given by eqn (1). Equation (1) is valid under the assumptions that the particles are arranged in a regular grid. In addition, the fraction of radiation transmitted through the particle layer is assumed equal to the void fraction (ϵ_f), and scattering is not present ($\sigma_s = 0$), Shin and Choi [1]. The limitations of eqn (1) are that particles are not arranged so ideally in a real bed, the void fraction may change over the layer of particles, and the equation does not say anything about the emissivity of the particles. The advantage of eqn (1) is that it is stable, Shin and Choi [1].

$$\begin{aligned} \kappa + \sigma_s = \kappa &= -\frac{1}{s} \cdot \text{Ln} \left(\frac{I_{\text{trans}}}{I_{\text{in}}} \right) = -\frac{1}{d_p} \cdot \text{Ln} \left(\frac{I_{\text{in}} \epsilon_f}{I_{\text{in}}} \right) \Rightarrow \\ \kappa &= -\frac{1}{d_p} \cdot \text{Ln}(\epsilon_f) \end{aligned} \quad (1)$$

Another simple but more accurate way to predict not only the large particles absorption coefficient, but also their scattering coefficient is given by eqns (2) and (3), Nilsson and Sundén in [2]. Equation (3) also includes the emissivity (ϵ) of the particles and allows for no ideal arrangement of opaque particles. Equation (3) also includes dependent scattering and absorption through a scaling factor (S_R), given by eqn (2). Then the scattering and absorption coefficients of large particles can be expressed by eqn (3). Thus the extinction coefficient ($\beta = \sigma_s + \kappa$) resulting from eqn (3) is only related to the porosity of the bed and the size of the particles, and through inspection of eqn (1) one can see that the same is true for that equation. Further, both eqns (1) and (3) have dependence on ($1/d_p$). Let us assume that the porosity of the bed varies between 0.45 and 0.5, and that the particle emissivity is equal to 0.75 (emissivity of char).

$$\begin{cases} S_R = 1.0 + 1.84 \cdot (1 - \epsilon_f) - 3.15 \cdot (1 - \epsilon_f)^2 + 7.20 \cdot (1 - \epsilon_f)^3 \\ \epsilon_f \geq 0.3 \end{cases} \quad (2)$$

$$\begin{cases} \sigma_s = 1.5 \cdot (1 - \varepsilon) \cdot (1 - \varepsilon_f) \cdot S_R / d_p \\ \kappa = 1.5 \cdot \varepsilon \cdot (1 - \varepsilon_f) \cdot S_R / d_p \end{cases} \quad (3)$$

From Table 1 one observes that for the porosities chosen and the assumed emissivity, the absorption coefficient given by eqn (1) is 39.4% to 42.8% smaller than the values given by eqn (3). Keep in mind that the influence of the particle diameter is the same in eqn (1) and eqn (3), so the particle diameter chosen in Table 1 does not matter, which also can be observed. Depending on the value of the porosity, the absorption coefficient in eqn (1) should be multiplied by a factor between 1.65 and 1.75 in order to obtain a better prediction of its value. A value of 1.70 is chosen here, and this will give the expression in eqn (4). The scattering coefficients of the particles are now easily gained by dividing the absorption coefficient in eqn (4) by 3. The factor 3 is a result of the emissivity chosen. Similar expressions can easily be obtained for other void fractions and emissivities.

$$\begin{cases} \kappa = -\frac{1.70}{d_p} \cdot \text{Ln}(\varepsilon_f) \\ \sigma_s = \frac{\kappa \cdot (1 - \varepsilon)}{\varepsilon} = \frac{\kappa}{3} \end{cases} \quad 0.45 \leq \varepsilon_f \leq 0.50 \quad \varepsilon = 0.75 \quad (4)$$

Table 1: Comparison between eqns (1) and (3).

$\kappa_1 = \kappa_{\text{eqn (1)}} \text{ and } \kappa_3 = \kappa_{\text{eqn (3)}}$							
ε_f [-]	d_p [m]	κ_1 [m^{-1}]	S_R [-]	$\sigma_{s,\text{eqn (3)}}$ [m^{-1}]	κ_3 [m^{-1}]	$\beta_{\text{eqn (3)}}$ [m^{-1}]	$(\kappa_1 - \kappa_3) / \kappa_3$
0.5	0.015	46.21	2.03	25.41	76.22	101.63	-0.394
0.5	0.02	34.66	2.03	19.05	57.16	76.22	-0.394
0.5	0.025	27.73	2.03	15.24	45.73	60.98	-0.394
0.45	0.015	53.23	2.26	31.03	93.10	124.14	-0.428
0.45	0.02	39.93	2.26	23.28	69.83	93.10	-0.428
0.45	0.025	31.94	2.26	18.62	55.86	74.48	-0.428

3 Gas absorption coefficients

An equation, eqn (5), has lately been applied in some investigations, e.g., Porterie and Loraud [3] and Al-Omari et al. [4]. Equation (5) is a combination of the empirical formula by Kent and

Honnery [5] for the soot, and that by Magnussen and Hjertager [6] for the gas. The part predicting the soot absorption coefficient is acceptable, but the part predicting the gas absorption gives too low values. In Table 2 a few cases are compared. From Table 2 one can see that at high values of the temperature, the mean beam length, and the concentrations of CO₂ and H₂O, a better agreement between the values predicted by the exponential wide band model (EWBM) and those given by eqn (5) is achieved.

$$\kappa = 0.1 \cdot (X_{\text{CO}_2} + X_{\text{H}_2\text{O}}) + 1862 \cdot f_v \cdot T \quad (5)$$

Table 2: Gas absorption coefficient (no soot present, $f_v = 0$).

Case	1	2	3	4	5	6	7	8	9	10	11
T [K]	1000	1000	1000	500	1500	1500	1500	1500	1500	1500	2500
L_m [m]	0.1	1	10	10	10	10	10	10	10	10	10
X_{CO_2} [%]	0.1	0.1	0.1	0.1	0.1	0.05	0.1	0.1	0.15	0.15	0.15
$X_{\text{H}_2\text{O}}$ [%]	0.2	0.2	0.2	0.2	0.2	0.2	0.1	0.3	0.2	0.3	0.3
EWBM	1.23	0.37	0.082	0.083	0.064	0.063	0.053	0.071	0.062	0.072	0.043
Eqn (5)	0.03	0.03	0.03	0.03	0.03	0.025	0.02	0.04	0.025	0.045	0.045
Error	-98%	-92%	-63%	-64%	-53%	-60%	-62%	-44%	-60%	-37%	-4.4%

Thus, eqn (5) should only be used when the mentioned criteria are fulfilled. It is well known that a local absorption coefficient (based on the mean beam length of a control volume) gives a better prediction, than a global absorption coefficient does (based on a mean beam length of the hole furnace), Liu et al. [7]. Therefore, the use of eqn (5) is not recommended as it comes to the gas part. Further, it is not easy to predict a temperature valid for the furnace as a whole. Instead, the use of the EWBM can be an alternative, because local temperatures and local mean beam lengths are used in the prediction of the absorption coefficient. Further, not only CO₂ and H₂O may be treated, but also CO and CH₄. CO₂, H₂O, CO and CH₄ are gases present in combustion of biofuels, and this is the reason why they are treated here. In the EWBM only three parameters are needed, i.e., α (integrated band intensity), β (line-width-to spacing parameter), and ω (bandwidth). The use of the EWBM may seem complicated due to the involved expressions given to calculate α and β , see eqns (6) and (7) below. Further, the infinite upper limits in the summations contribute to increase the computational time. In reality the upper limits are, e.g., $v_k = 15$. An

upper limit of 10 in the sums gives acceptable results, as far as accuracy is concerned. A way to reduce the complexity and the computational needs, are to give polynomial fits of α/α_0 and γ/γ_0 for each and every band as a function of temperature ($\omega/\omega_0 = \sqrt{T/T_0}$, so no polynomial is needed for ω/ω_0). This is possible, because the given values for α/α_0 and γ/γ_0 for each band behave in a nice way, see Figures 1 to 9. The polynomial fits need to be carried out only once, and this will reduce the mathematical operations, which in turn will reduce the computational time and the complexity. The polynomials have a form given by eqns (8) and (9), and the constants used are given in the appendix. Lower grade polynomials (e.g., 4), would even more accelerate the predictions and simplify the use of the EWBM, but this will give errors of the order of 10% for some cases, Lallemand and Weber [8].

$$\left\{ \begin{array}{l} \alpha(T) = \alpha_0 \cdot \frac{\Psi^*(T)}{\Psi^*(T_0)} \\ \Psi^*(T) = \left(1 - e^{-\sum_{k=1}^m u_k \delta_k} \right) \frac{\prod_{k=1}^m \sum_{v_k=v_{0,k}}^{\infty} \frac{(v_k + g_k + |\delta_k| - 1)!}{(g_k - 1)! \cdot v_k!} e^{-u_k v_k}}{\prod_{k=1}^m \sum_{v_k=0}^{\infty} \frac{(v_k + g_k - 1)!}{(g_k - 1)! \cdot v_k!} e^{-u_k v_k}} \end{array} \right. \quad (6)$$

$$\left\{ \begin{array}{l} \beta(T) = \gamma \cdot P_e = \gamma_0 \cdot \sqrt{\frac{T_0}{T}} \cdot \frac{\Phi(T)}{\Phi(T_0)} \cdot P_e \\ \Phi(T) = \frac{\left\{ \prod_{k=1}^m \sum_{v_k=v_{0,k}}^{\infty} \frac{(v_k + g_k + |\delta_k| - 1)!}{(g_k - 1)! \cdot v_k!} e^{-u_k v_k} \right\}^2}{\prod_{k=1}^m \sum_{v_k=v_{0,k}}^{\infty} \frac{(v_k + g_k + |\delta_k| - 1)!}{(g_k - 1)! \cdot v_k!} e^{-u_k v_k}} \end{array} \right. \quad (7)$$

$$\frac{\alpha}{\alpha_0} = a_0 + a_1 \cdot T + a_2 \cdot T^2 + a_3 \cdot T^3 + a_4 \cdot T^4 + a_5 \cdot T^5 + a_6 \cdot T^6 \quad (8)$$

$$\frac{\gamma}{\gamma_0} = b_0 + b_1 \cdot T + b_2 \cdot T^2 + b_3 \cdot T^3 + b_4 \cdot T^4 + b_5 \cdot T^5 + b_6 \cdot T^6 \quad (9)$$

4 Results and discussion

For 145152 different combinations of the temperature, mean beam length and concentrations of H₂O, CO₂, CO and CH₄, absorption coefficients were calculated using the block approximation proposed by Edwards [9].

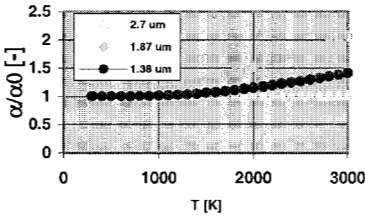


Figure 1: α/α_0 v.s. T for H₂O.

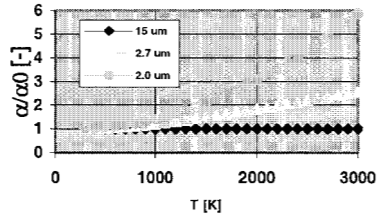


Figure 2: α/α_0 v.s. T for CO₂.

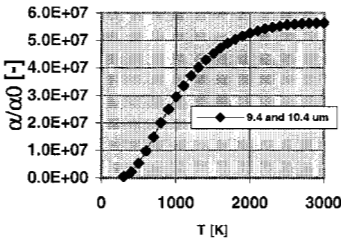


Figure 3: α/α_0 v.s. T for CO₂.

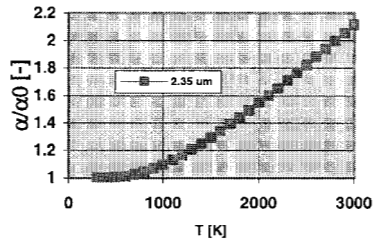


Figure 4: α/α_0 v.s. T for CO.

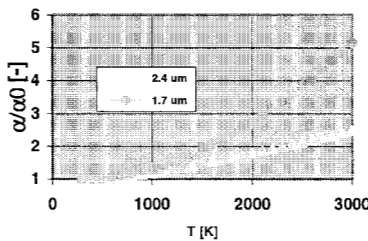


Figure 5: α/α_0 v.s. T for CH₄.

The mean time to calculate one value of the absorption coefficient, using the polynomial fits given, is 71 μ s. Corresponding computational times are 996 μ s and 2718 μ s, if one uses eqns (6) and (7) with upper limits of 10 and 25, respectively, in the summations.

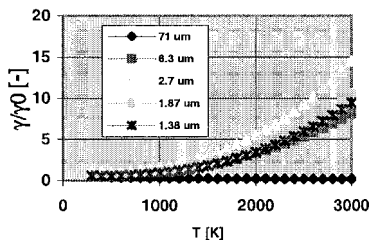


Figure 6: γ/γ_0 v.s. T for H₂O.

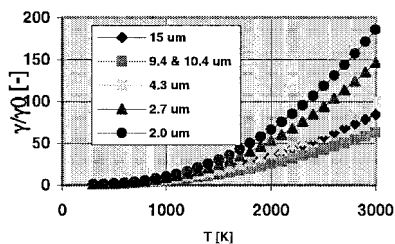


Figure 7: γ/γ_0 v.s. T for CO₂.

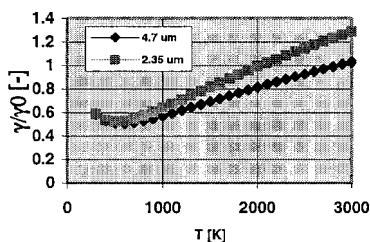


Figure 8: γ/γ_0 v.s. T for CO.

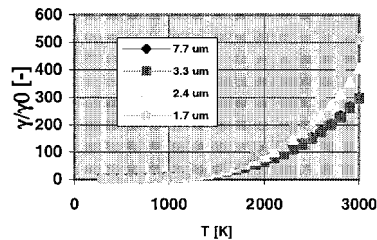


Figure 9: γ/γ_0 v.s. T for CH₄.

The maximal error $((\kappa_{\text{poly}} - \kappa_{\text{EWBM}}) / \kappa_{\text{EWBM}})$ occurs at low temperatures. In Table 3 some cases at low temperatures are given with their accompanied errors. The maximal error found is around 0.25 %. The general trend is that the errors will decrease when the temperature increases, as is evident from Tables 3 and 4.

Table 3: Error between the absorption coefficient given by the polynomial fits and the EWBM, at 500 K.

$X_{\text{H}_2\text{O}} = 0.05$	$L_m = 2 \text{ m}$	$T = 500 \text{ K}$	Error = 0.00102
$X_{\text{CO}_2} = 0.15$	$L_m = 10 \text{ m}$	$T = 500 \text{ K}$	Error = 0.00168
$X_{\text{CO}} = 0.05$	$L_m = 2 \text{ m}$	$T = 500 \text{ K}$	Error = 0.00229
$X_{\text{CH}_4} = 0.15$	$L_m = 0.2 \text{ m}$	$T = 500 \text{ K}$	Error = 0.00214

Table 4: Error between the absorption coefficient given by the polynomial fits and the EWBM, at 1000 K.

$X_{\text{H}_2\text{O}} = 0.05$	$L_m = 2 \text{ m}$	$T = 1000 \text{ K}$	Error = -0.000005
$X_{\text{CO}_2} = 0.15$	$L_m = 10 \text{ m}$	$T = 1000 \text{ K}$	Error = -0.000184
$X_{\text{CO}} = 0.05$	$L_m = 2 \text{ m}$	$T = 1000 \text{ K}$	Error = -0.000136
$X_{\text{CH}_4} = 0.15$	$L_m = 0.2 \text{ m}$	$T = 1000 \text{ K}$	Error = -0.000080

5 Conclusions

The expression for large particles given by Shin and Choi, i.e., eqn (1), is improved so that multiple scattering is taken into consideration. Further, the belonging scattering coefficient is presented. Magnussen and Hjertager presented an expression for the gas absorption coefficient, see eqn (5). The gas term, in eqn (5), only gives acceptable results when the temperatures are high, the concentrations are high and when the mean beam lengths are large. Finally, a simplification of the exponential wide band model is presented in forms of polynomial fits. The polynomials decrease the computational time by a factor of at least ten, but with almost no change in the calculated values of the absorption coefficient.

Notation

Table 5: Nomenclature.

d_p [m]	particle diameter	α [m/kg]	integrated band intensity
f_v [-]	volume fraction	β [1/m]	extinction coefficient
g_k [-]	degeneracy	β [-]	line overlap parameter
I [W/m ² /Sr]	intensity	δ_k [-]	change in v_k
L_m [m]	mean beam length	ε [-]	emissivity
P_e [-]	effective pressure	ε_f [-]	void fraction
s [m]	geometric path length	Φ [-]	see eqn (7)
S_R [-]	scaling factor	γ [-]	line overlap parameter
T [K]	temperature	κ [1/m]	absorption coefficient
u_k [-]	transition wave number	λ [m]	wavelength
v_k [-]	quantum number	σ_s [1/m]	scattering coefficient
X_{CO_2} [-]	molar fraction CO ₂	ω [1/m]	band width
X_{H_2O} [-]	molar fraction H ₂ O	ψ^* [-]	see eqn (6)

Acknowledgement

The authors kindly acknowledge the financial support from SSF (Foundation of Strategical Research) in Sweden via the CECOST program.

References

- [1] Shin, D. & Choi, S., The combustion of simulated waste particles in a fixed bed. *Combustion and Flame*, **121**, pp. 167-180, 2000.
- [2] Sundén, B. & Brebbia, C. A., (eds). *Advanced Computational Methods in Heat Transfer VI*, WIT Press: Southampton and Boston, pp. 203-211, 2000.
- [3] Porterie, B. & Loraud, J. C., The prediction of some compartment fires. Part 1: mathematical model and numerical method. *Numerical Heat Transfer Part A*, **39**, pp.139-153, 2001.
- [4] Al-Omari, S.-A. B., Kawajiri, K. & Yonesawa, T., Soot processes in a methane-fueled furnace and their impact on radiation heat transfer to furnace walls. *Int. J. Heat Mass Transfer*, **44**, pp. 2567-2581, 2001.
- [5] J. H. Kent & D. R. Honnery, A soot formation rate map for laminar ethylene diffusion flame. *Combustion and Flame*, **79**, pp. 287-298, 1990.
- [6] B. F. Magnussen & B. H. Hjertager, On mathematical modelling of turbulent combustion with special emphasis on soot formation and combustion. *16th Symposium (International) on Combustion*, The Combustion Institute, Pittsburgh, PA, pp. 719-729, 1976.
- [7] Liu, F., Gülder, Ö. L., Smallwood, G. J. & Ju, Y., Non-grey gas radiative transfer analyses using the statistical narrow-band model. *Int. J. Heat Mass Transfer*, **41(14)**, pp. 2227-2236, 1998.
- [8] Lallemand, N. & Weber, R., A computationally efficient procedure for calculating gas radiative properties using the exponential wide band model. *Int. J. Heat Mass Transfer*, **39(15)**, pp. 3273-3286, 1996.
- [9] Edwards, D. K., Molecular gas band radiation. *Advances in heat transfer, Volume 12*, ed. T. F. Irvine & J. P. Hartnett, Academic Press: New York, San Francisco and London, pp. 115-193, 1976.

Appendix

Tables 6 to 9 in the appendix below give the constants a_0 to a_6 and b_0 to b_6 , for each band for the gases H_2O , CO_2 , CO and CH_4 .

Table 6: H₂O, polynomial coefficients for α/α_0 and γ/γ_0 .

λ	α_0	a_0	a_1	a_2	a_3	a_4	a_5	a_6
$71.0 \cdot 10^{-6}$	$44205 \cdot 10^3$	1	0	0	0	0	0	0
$6.30 \cdot 10^{-6}$	$41.2 \cdot 10^5$	1	0	0	0	0	0	0
$2.70 \cdot 10^{-6}$	$24.89 \cdot 10^3$	1.000657054471	$-4.200291900245 \cdot 10^{-6}$	$7.765786982639 \cdot 10^{-9}$	$-3.105385851234 \cdot 10^{-12}$	$6.497085910815 \cdot 10^{-16}$	$-5.531663970133 \cdot 10^{-20}$	0
$1.87 \cdot 10^{-6}$	$3 \cdot 10^5$	1.032648716046	$-2.054835125613 \cdot 10^{-4}$	$3.462276437202 \cdot 10^{-7}$	$-4.207905957343 \cdot 10^{-11}$	$-2.347425688468 \cdot 10^{-14}$	$9.800185095492 \cdot 10^{-18}$	$-1.108705542952 \cdot 10^{-21}$
$1.38 \cdot 10^{-6}$	$2.5 \cdot 10^3$	0.9853969321373	$1.022199322435 \cdot 10^{-4}$	$-2.466320864862 \cdot 10^{-7}$	$2.445995079217 \cdot 10^{-10}$	$-9.061830586663 \cdot 10^{-14}$	$1.592910281252 \cdot 10^{-17}$	$-1.096801078112 \cdot 10^{-21}$
λ	γ_0	b_0	b_1	b_2	b_3	b_4	b_5	b_6
$71.0 \cdot 10^{-6}$	0.14311	0.9619429626087	$-1.875417914377 \cdot 10^{-3}$	$2.433591152118 \cdot 10^{-6}$	$-1.809963947943 \cdot 10^{-9}$	$7.564161700224 \cdot 10^{-13}$	$-1.649605792234 \cdot 10^{-16}$	$1.458200070423 \cdot 10^{-20}$
$6.30 \cdot 10^{-6}$	0.09427	0.9054355976493	$-1.752321759686 \cdot 10^{-3}$	$3.085210500315 \cdot 10^{-6}$	$-1.970610940622 \cdot 10^{-9}$	$9.241306888868 \cdot 10^{-13}$	$-2.080397889389 \cdot 10^{-16}$	$1.867096830920 \cdot 10^{-20}$
$2.70 \cdot 10^{-6}$	0.13219	1.669891283545	$-3.301207425788 \cdot 10^{-3}$	$5.355977237715 \cdot 10^{-6}$	$-3.432978832931 \cdot 10^{-9}$	$1.622776873204 \cdot 10^{-12}$	$-3.601985006551 \cdot 10^{-16}$	$3.198855795808 \cdot 10^{-20}$
$1.87 \cdot 10^{-6}$	0.08169	0.9051626779327	$-1.740865411243 \cdot 10^{-3}$	$3.021178212792 \cdot 10^{-6}$	$-1.876265416581 \cdot 10^{-9}$	$9.428747431030 \cdot 10^{-13}$	$-2.140128155785 \cdot 10^{-16}$	$1.919655080005 \cdot 10^{-20}$
$1.38 \cdot 10^{-6}$	0.11628	0.9353335664035	$-1.860052190363 \cdot 10^{-3}$	$2.974373557327 \cdot 10^{-6}$	$-1.892337104956 \cdot 10^{-9}$	$9.336168458108 \cdot 10^{-13}$	$-2.084238794098 \cdot 10^{-16}$	$1.847115901794 \cdot 10^{-20}$

Table 7: CO, polynomial coefficients for α/α_0 and γ/γ_0 .

λ	α_0	a_0	a_1	a_2	a_3	a_4	a_5	a_6
$4.70 \cdot 10^{-6}$	$20.9 \cdot 10^3$	1	0	0	0	0	0	0
$2.35 \cdot 10^{-6}$	$0.14 \cdot 10^5$	1.020285794281	$-7.486578190246 \cdot 10^{-3}$	$-6.818529849087 \cdot 10^{-8}$	$4.095847899995 \cdot 10^{-10}$	$-2.479682147110 \cdot 10^{-13}$	$6.336234156564 \cdot 10^{-17}$	$-6.088738783077 \cdot 10^{-21}$
λ	γ_0	b_0	b_1	b_2	b_3	b_4	b_5	b_6
$4.70 \cdot 10^{-6}$	0.07506	0.9806280043466	$-2.195755290821 \cdot 10^{-3}$	$3.661010331308 \cdot 10^{-6}$	$-2.831451057364 \cdot 10^{-9}$	$1.193397045067 \cdot 10^{-12}$	$-2.604132146506 \cdot 10^{-16}$	$2.298081740722 \cdot 10^{-20}$
$2.35 \cdot 10^{-6}$	0.16758	0.9897071095516	$-2.294310251228 \cdot 10^{-3}$	$3.971164022386 \cdot 10^{-6}$	$-3.051679360365 \cdot 10^{-9}$	$1.276040452656 \cdot 10^{-12}$	$-2.767207734015 \cdot 10^{-16}$	$2.430808279383 \cdot 10^{-20}$

Table 8: CO₂, polynomial coefficients for α/α_0 and γ/γ_0 .

λ	α_0	a_0	a_1	a_2	a_3	a_4	a_5	a_6
$15.0 \cdot 10^{-6}$	$19 \cdot 10^5$	0.9997704143705	$1.186219322425 \cdot 10^{-6}$	$-1.914996802435 \cdot 10^{-9}$	$1.111174210505 \cdot 10^{-12}$	$-1.112764768357 \cdot 10^{-16}$	$-5.574880299925 \cdot 10^{-20}$	0
$10.4 \cdot 10^{-6}$	$2.47 \cdot 10^4$	$1.499832445008 \cdot 10^7$	$-1.228811743229 \cdot 10^5$	$3.215060620254 \cdot 10^2$	-0.2827399874965	$1.228837206033 \cdot 10^{-4}$	$-2.674569744386 \cdot 10^{-8}$	$2.326766029910 \cdot 10^{-12}$
$9.40 \cdot 10^{-6}$	$2.48 \cdot 10^4$	$1.499832445008 \cdot 10^7$	$-1.228811743229 \cdot 10^5$	$3.215060620254 \cdot 10^2$	-0.2827399874965	$1.228837206033 \cdot 10^{-4}$	$-2.674569744386 \cdot 10^{-8}$	$2.326766029910 \cdot 10^{-12}$
$4.30 \cdot 10^{-6}$	$110 \cdot 10^5$	1	0	0	0	0	0	0
$2.70 \cdot 10^{-6}$	$4 \cdot 10^3$	1.052660862699	$-3.541572635956 \cdot 10^{-4}$	$6.730058412805 \cdot 10^{-7}$	$-1.820549476875 \cdot 10^{-10}$	$2.893734499076 \cdot 10^{-13}$	$8.887217837865 \cdot 10^{-18}$	$-1.323920578508 \cdot 10^{-21}$
$2.00 \cdot 10^{-6}$	$0.066 \cdot 10^3$	1.081405501888	$-5.661058083657 \cdot 10^{-4}$	$1.098741988368 \cdot 10^{-6}$	$-2.761936912346 \cdot 10^{-10}$	$7.866983406224 \cdot 10^{-14}$	$-1.139910118023 \cdot 10^{-17}$	$6.334505989706 \cdot 10^{-22}$

λ	γ_0	b_0	b_1	b_2	b_3	b_4	b_5	b_6
$15.0 \cdot 10^{-6}$	0.06157	0.7433857428294	$-2.582182355382 \cdot 10^{-4}$	$5.634557756406 \cdot 10^{-6}$	$-8.458693494915 \cdot 10^{-11}$	$2.168044728028 \cdot 10^{-12}$	$-8.592415495996 \cdot 10^{-16}$	$9.474528705179 \cdot 10^{-20}$
$10.4 \cdot 10^{-6}$	0.04017	0.7508514387089	$-1.122382442765 \cdot 10^{-4}$	$3.143120887759 \cdot 10^{-6}$	$1.423380802994 \cdot 10^{-9}$	$5.032874657862 \cdot 10^{-13}$	$-2.749589305882 \cdot 10^{-16}$	$3.012559784622 \cdot 10^{-20}$
$9.40 \cdot 10^{-6}$	0.11888	0.7508514387089	$-1.122382442765 \cdot 10^{-4}$	$3.143120887759 \cdot 10^{-6}$	$1.423380802994 \cdot 10^{-9}$	$5.032874657862 \cdot 10^{-13}$	$-2.749589305882 \cdot 10^{-16}$	$3.012559784622 \cdot 10^{-20}$
$4.30 \cdot 10^{-6}$	0.24723	0.7576800254755	$-1.940980156222 \cdot 10^{-4}$	$3.477651631187 \cdot 10^{-6}$	$1.948642691580 \cdot 10^{-9}$	$1.289458950808 \cdot 10^{-12}$	$-5.238525787875 \cdot 10^{-16}$	$5.188387438949 \cdot 10^{-20}$
$2.70 \cdot 10^{-6}$	0.13341	0.7394110772285	$-1.316813790731 \cdot 10^{-4}$	$3.288243344714 \cdot 10^{-6}$	$3.683030655373 \cdot 10^{-9}$	$1.859883883234 \cdot 10^{-12}$	$-7.739168369132 \cdot 10^{-16}$	$7.496872348807 \cdot 10^{-20}$
$2.00 \cdot 10^{-6}$	0.39305	0.7118728848707	$5.829511924208 \cdot 10^{-5}$	$2.589915732862 \cdot 10^{-6}$	$5.903803964989 \cdot 10^{-9}$	$1.922599670843 \cdot 10^{-12}$	$-8.827696159419 \cdot 10^{-16}$	$8.361391876036 \cdot 10^{-20}$

Table 9: CH₄, polynomial coefficients for α/α_0 and γ/γ_0 .

λ	α_0	a_0	a_1	a_2	a_3	a_4	a_5	a_6
$7.70 \cdot 10^{-6}$	$28 \cdot 10^5$	1	0	0	0	0	0	0
$3.30 \cdot 10^{-6}$	$46 \cdot 10^5$	1	0	0	0	0	0	0
$2.40 \cdot 10^{-6}$	$2.9 \cdot 10^5$	1.045202997465	$-3.271078702106 \cdot 10^{-4}$	$6.837363574125 \cdot 10^{-7}$	$-2.537054324990 \cdot 10^{-10}$	$5.214732074048 \cdot 10^{-14}$	$-4.793291435739 \cdot 10^{-18}$	$6.847027562987 \cdot 10^{-23}$
$1.70 \cdot 10^{-6}$	$0.42 \cdot 10^5$	1.073343847251	$-5.097567078337 \cdot 10^{-4}$	$9.969443038214 \cdot 10^{-7}$	$-2.890268618651 \cdot 10^{-10}$	$9.014257949786 \cdot 10^{-14}$	$-1.469814681733 \cdot 10^{-17}$	$9.685517032682 \cdot 10^{-22}$
λ	γ_0	b_0	b_1	b_2	b_3	b_4	b_5	b_6
$7.70 \cdot 10^{-6}$	0.08698	0.7542150303509	$-1.193060103611 \cdot 10^{-3}$	$3.962827099173 \cdot 10^{-6}$	$-2.151084109220 \cdot 10^{-9}$	$4.802290896290 \cdot 10^{-12}$	$-1.283528714603 \cdot 10^{-16}$	$-4.575824672631 \cdot 10^{-20}$
$3.30 \cdot 10^{-6}$	0.06973	0.8683857654479	$-1.991647643423 \cdot 10^{-3}$	$5.961412027376 \cdot 10^{-6}$	$-5.126680142390 \cdot 10^{-9}$	$6.358058942547 \cdot 10^{-12}$	$-5.503353018788 \cdot 10^{-16}$	$5.590320435871 \cdot 10^{-21}$
$2.40 \cdot 10^{-6}$	0.35429	0.8544061749554	$-1.976935744809 \cdot 10^{-3}$	$6.251095464397 \cdot 10^{-6}$	$-5.347999210178 \cdot 10^{-9}$	$6.848633020930 \cdot 10^{-12}$	$5.998696603502 \cdot 10^{-17}$	$-9.507615434908 \cdot 10^{-20}$
$1.70 \cdot 10^{-6}$	0.68598	0.8514318021353	$-2.090990605886 \cdot 10^{-3}$	$6.997177447921 \cdot 10^{-6}$	$-6.546828972440 \cdot 10^{-9}$	$8.423699570006 \cdot 10^{-12}$	$2.356332896046 \cdot 10^{-16}$	$-1.450881723267 \cdot 10^{-19}$